IEEE Access
Multidisciplinary | Rapid Review | Open Access Journal

SPECIAL SECTION ON POWER ELECTRONICS EMERGING TECHNOLOGIES FOR SUSTAINABLE ENERGY CONSERVATION

Received 7 April 2023, accepted 3 May 2023, date of publication 9 May 2023, date of current version 18 May 2023.

Digital Object Identifier 10.1109/ACCESS.2023.3274607

RESEARCH ARTICLE

A Complete Online Solution of Harmonic Elimination PWM Method Using Modified-Equilibrium Optimizer-Levenberg-Marquardt Algorithm

ABDUL MOEED AMJAD[1,2], KAMYAR MEHRAN[1], (Senior Member, IEEE), AND SHADY GADOUE[1]

[1]School of Electronic Engineering and Computer Science, Queen Mary University of London, E14NS London, U.K.
[2]Department of Electrical Engineering, COMSATS University Islamabad, Lahore Campus, Lahore 54000, Pakistan

Corresponding author: Abdul Moeed Amjad (abdulmoeed19@gmail.com)

This work was supported in part by the Higher Education Commission, Pakistan; and in part by the Queen Mary University of London, U.K.

ABSTRACT This paper proposes a novel online solution, i.e. Modified-Equilibrium Optimizer-Levenberg-Marquardt (M-EO-LM) algorithm, for the symmetric and asymmetric harmonic elimination pulse width modulation (HEPWM) methods of the modular multilevel cascaded converters. A detailed comparison of the proposed M-EO-LM algorithm with nine state-of-the-art algorithms is also presented for twenty-nine unimodal, multimodal and composite benchmark test functions. M-EO-LM has proven its effectiveness by outperforming these algorithms. EO algorithm is first introduced for the solution of HEPWM method. Its comparison with several state-of-the-art algorithms depicts its superiority; but it gets stuck in the local minima. Modified-EO (M-EO) solves the problem by enhancing its exploration ability, and is then attached to a rapid calculus-based LM method to form the novel M-EO-LM algorithm. M-EO-LM algorithm initiates the solution process by solving the HEPWM equations for nine angles ($N = 9$ and $0.78 \leq M \leq 6.86$) offline in only two iterations, depicting its remarkable convergence ability. Solution angles are then divided into several groups, serving as the search space for the online M-EO-LM algorithm. A comparison between HEPWM and nearest level modulation methods based on the output voltage THD values is provided to report the maximum number of solvable HEPWM angles for a complete online solution. These angles ($N = 8$ and $0.78 \leq M < 5.18$) are then solved online using the M-EO-LM algorithm. Comparing the computational times of the proposed online algorithm with differential evolution-Newton Raphson algorithm proves the rapid solution behavior of the M-EO-LM algorithm, validated through the simulation and real-time experimental results.

INDEX TERMS Harmonic elimination PWM, modular multilevel cascade converter, fundamental voltage control, harmonic control, equilibrium optimizer, Levenberg-Marquardt algorithm.

I. INTRODUCTION

Modular multilevel cascade converters (MMCCs) have become indispensable for electrical power systems due to their better harmonic behavior, better reliability and ability to produce medium and high voltage outputs [1], [2]. MMCCs are further divided into four categories based on the configuration of their sub-modules (SMs): single-star bridge cell (SSBC), single-delta bridge cell (SDBC), double-star chopper cell (DSCC), and double-star bridge cell (DSBC) [1]. SSBC-MMCC being the simplest, is chosen in the work and will be referred as MMCC (for simplicity) instead of the full form SSBC-MMCC. Three-phase structure of MMCC is depicted in Fig. 1(a). Each phase is comprised of

The associate editor coordinating the review of this manuscript and approving it for publication was Javier Moreno-Valenzuela.

'*N*' full-bridge (FB) SMs (Fig. 1(b)). Quarter-wave output phase voltage of MMCC is shown in Fig. 1(c). MMCCs are attached with certain demerits for instance, circulating currents, SM input voltage imbalance, output harmonics, etc. [2], [3], [4]; however, present study only focuses on the harmonic elimination from their output voltage using harmonic elimination pulse width modulation (HEPWM) method. HEPWM method surpasses its counterparts due to its low frequency operation, better harmonics profile and fundamental voltage control [5], [6], [7]. Several offline computing methods have been reported to solve the HEPWM equations [5], [6], [7], [8], [9], [10]. These methods can be categorized into two groups, namely calculus based algorithms and soft computing (SC) algorithms. Calculus based algorithms require a good initial guess, which should be closer to the global minimum. This initial guess is not always available for the transcendental HEPWM equations, leading to the discontinuities in the solution. Hence, a significant amount of research is carried out using SC methods, which include genetic algorithm (GA), particle swarm optimization (PSO), differential evolution (DE), flower pollination algorithm (FPA), etc. These algorithms employ the random search to track the global minima, and provide excellent offline solution to the HEPWM equations without requiring a good initial guess. SC algorithm based offline solution of HEPWM equations are widely discussed in the literature [8], [9], [10]. Solution angles obtained offline are stored in the form of look-up tables (LUTs) for real-time application. However, these LUTs not only present critical need of large memory but also fail to address the dynamic behavior of the system operating on a large range of M [11]. Hence, real-time implementation of these algorithms is not always realistic. Recently, various online solution techniques of HEPWM method have been presented to address these problems [11], [12], [13], [14], [15], [16], [17].

In [11], a real-time solution of HEPWM is provided by converting its mathematical model into a control system model. The method avoids computationally burdened calculations; but, is presented for three SMs only. Moreover, as it requires a LUT, integral controllers and a decoupled controller for its working, the complexity of the control system will increase for higher number of SMs. A fusion of artificial neural networks (ANNs) and Quasi-Newton algorithm is proposed in [12] to solve the HEPWM method in real-time. ANNs generate the sub-optimal initial guess, which are utilized by the Quasi-Newton algorithm to calculate the HEPWM switching angles during real-time operations. However, presence of several discontinuities pose serious challenges for the algorithm, whose performance is presented for limited values of M. Moreover, the solution process is slow and requires several fundamental time periods. A novel homotopy perturbation method is presented in [13] to solve the HEPWM method. However, the solution process is not fast enough as it requires computational time of tens of fundamental time period. A rapid online differential

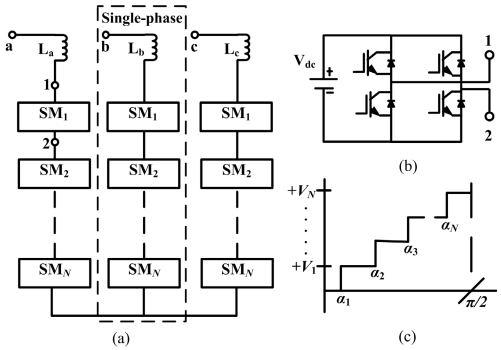

FIGURE 1. Representation of (a) Modular multilevel cascade converter. (b) Full-bridge sub-module. (c) Quarter-wave single-phase output voltage.

evolution-Newton Raphson (DE-NR) algorithm is presented in [14] to solve HEPWM equations. DE-NR algorithm is a combination of DE and NR algorithms. It simultaneously exploits the excellent global search ability of DE and rapid convergence behavior of NR algorithms to obtain the solution. Solution process starts by optimizing a particular set of population vectors using the DE algorithm. These vectors are then utilized as the initial guess for the NR algorithm to locate the global minima. Solution process is completed in less than a fundamental time period, which depicts the faster behavior of DE-NR algorithm. However, in these algorithms [12], [13], [14], input voltages of SMs are considered equal (termed as symmetric HEPWM), which contradicts the real-time operation of MMCCs where dynamic operating conditions lead to unequal magnitude of input voltage sources (asymmetric HEPWM). Hence, these methods are prone to underperformance, and their application for the online solution of asymmetric HEPWM needs to be discussed.

Few works are reported to target the online solution of asymmetric HEPWM [15], [16], [17]. A combination of genetic algorithm (GA) and ANNs is utilized in [15] to solve asymmetric HEPWM method for five angles. Offline calculations are performed by GA to obtain a LUT, which is then utilized to train ANNs for the real-time calculations. A well trained ANN system abolishes the requirement of LUTs during the real-time operation. However, GA does not always produce continuous HEPWM solution angle trajectories, which leads to the substandard training of ANNs for certain values of M. Hence, sub-optimal results are produced by the ANNs during the online operation for these values of M, which deteriorates the efficient working of the MMCC based power systems. Furthermore, the memory requirement for the storage of offline results in the form of LUT to produce the near to accurate results by ANNs is quite high. Hence, the work has reported the online solution of HEPWM method for the variation of a single input voltage only, which limits the real-time applications of the proposed method. In addition, computational time analysis and the online solution of HEPWM method for a wide range of M is not discussed. A modified version of HEPWM named as SHE-PAM is

presented in [16] for the real-time operation. The method follows the principle of amplitude modulation and requires specific values of input voltages for a particular value of M. As these input values may not always be available, so the method cannot be applied efficiently for the real-time operation of MMCCs. An online stochastic configuration network Levenberg-Marquardt (SCN-LM) solution algorithm for asymmetric HEPWM is presented in [17]. It requires offline training and tuning of parameters of SCN, which is based on the pre-calculated HEWPM angles. The parameter values are then employed online by SCN to generate initial guess for the LM algorithm, which produces the final solution. Asymmetric solution of three HEPWM angles is presented, but its application for larger number of angles is not reported. In short, current online solution methods either produce sub-optimal results, are not fast enough or their application is limited to the small number of HEPWM angles. To fill this niche, a resolute online modified-Equilibrium Optimizer-Levenberg Marquardt (M-EO-LM) algorithm is proposed for symmetric and asymmetric HEPWM methods. Present work is consisted of the offline and online solution of HEPWM equations using M-EO-LM algorithm, and the major contributions include:

- Development and application of a novel M-EO-LM algorithm for the solution of optimization problems.
- Continuous offline solution of symmetric and asymmetric HEPWM equations for $0.78 \leq M \leq 6.86$ in only two iterations, with desired output voltage fundamental component and harmonics control.
- Realization of the rapid and complete online solution of symmetric and asymmetric HEPWM equations.

First, offline solution process starts with the application and modification of a novel EO algorithm for the HEPWM method. It is named as modified-EO (M-EO) and its superiority is established by comparing it with four different state-of-the-art algorithms. M-EO is then combined with the LM algorithm to form a novel M-EO-LM algorithm for the rapid solution of HEPWM method. Offline results are then summarized into a compact table, which replaces the memory burdened LUT for the online solution. In addition, a comparison of HEPWM and nearest level modulation (NLM) methods is provided to obtain the maximum values of N and M for the complete online solution of HEPWM methods using the M-EO-LM algorithm.

Second part of the work reports online implementation of the M-EO-LM algorithm for HEPWM method. Compact table obtained during the offline solution is utilized to present a novel online solution framework for the symmetric and asymmetric HEPWM methods. Rapid convergence of the online M-EO-LM algorithm compared with the online DE-NR algorithm [14] is also established. Simulation and online experimental results are presented, which verify the applicability of the M-EO-LM algorithm for the online solution of HEPWM method. As the objective is to introduce the rapid online solution algorithm (M-EO-LM) for the HEPWM method, application of the proposed algorithm for calculating the HEPWM angles during the dynamic changes in the values of M is only considered in this work. Its application for the voltage control, current control, circulating current control and voltage ripple control, etc. of MMCCs will be discussed in the future studies.

The paper is organized as follows: Section II explains the symmetric and asymmetric HEPWM methods followed by the short description of NLM method in section III. A comprehensive description and working of the proposed online algorithm (M-EO-LM) is presented in section IV, which is validated by the simulation and experimental results in sections V and VI respectively. The article is concluded in section VII.

II. HARMONIC ELIMINATION PWM

Control of the output fundamental voltage component and the removal of harmonics from the output voltage of MMCCs using HEPWM method requires the solution of a computationally burdened set of transcendental equations [5], [6], [7]. Several forms of HEPWM method (unified HEPWM [17], [18], SHE-PAM [16], non-fundamental switching HEPWM method [9], etc.) are reported in the literature but the current work targets the conventional fundamental switching frequency HEPWM method (SMs are switched with the fundamental frequency of 50 or 60 Hz). However, the proposed online solution algorithm is equally applicable to all forms of the HEPWM method. Generalized mathematical model of the HEPWM method is presented by (1) to (3) with the fitness function (4), provided the constraints of (5) are observed.

$$\sum_{i=1}^{N} V_i' \cos \alpha_i - M = \epsilon_1 \tag{1}$$

$$\sum_{i=1}^{N} V_i' \cos k\alpha_i = \epsilon_k \tag{2}$$

where $k = \{5, 7, \ldots, 3N-1\}$ or $\{5, 7, \ldots, 3N-2\}$ for even/odd value of N, and M controls the magnitude of fundamental component (V_f) of the output voltage using (3).

$$M = \pi |V_f| / 4V_{\text{dc}}, \quad 0 < M \leq N \tag{3}$$

Harmonics produced in the output voltage of MMCCs have detrimental effect on the system performance as they generate power losses, unwanted switching of protection devices, power quality issues, etc. To limit the harmful effects of harmonics, THD of the output voltage is required to be controlled to a certain level as recommended by the IEEE-Standard 519-2014 [19]. Therefore, the fitness function used in this study is focused on limiting the THD of the output voltage, which is described below:

$$f(\alpha) = \sqrt{(\epsilon_1)^2 + (\epsilon_5)^2 + \ldots + (\epsilon_k)^2} \tag{4}$$

$$0 < \alpha_1 < \alpha_2 < \ldots < \alpha_N < \pi/2 \tag{5}$$

Here V_{dc}, ϵ and $f(\alpha)$ represent the input dc voltage, calculation error and the fitness function value respectively, while V_i' $(i = 1, 2, \ldots, N)$ represents the normalized magnitude

of input voltages ($V_1, V_2, \ldots, V_N$) with respect to V_{dc}. Symmetric HEPWM method (when all input voltages are equal) being the simplest, remains the target of most publications, and is commonly referred as HEPWM. However, asymmetric HEPWM method (when at least one input voltage is different) encompasses the practical working conditions, and is imperative for the real-time operation of MMCC based power systems. Present work targets both categories to provide a complete online solution of the HEPWM method. As triplen harmonics are automatically removed in a stable three-phase system, so (1) to (5) are solved for the first N non-triplen harmonics. The first non-eliminated harmonics component will be $(3N+1)^{th}$ or $(3N+2)^{th}$ for even or odd number of N respectively.

Since HEPWM equations are transcendental in nature, the solution complexity and the computational burden increase with the increase in the value of N, which limits its real-time applications for MMCCs with large values of N. NLM has appeared as an alternative, but it suffers with poor harmonics profile for smaller values of N. Hence, the work focuses on the online solution of HEPWM equations till a suitable value of N, beyond which, NLM can be applied for the real-time operation. A brief description of NLM is provided below.

III. NEAREST LEVEL MODULATION

NLM method is a fundamental switching frequency method, and has found several online applications in high voltage DC (HVDC) systems due to its simple architecture and low computational burden [20], [21], [22]. It requires the solution of (6) for N number of angles.

$$\alpha_i = \sin^{-1}[\pi(i-0.5)/(4M)], \quad i = 1, 2, \ldots, N \tag{6}$$

Despite its simple construction, harmonics profile attached to the output voltage of MMCCs (generated by NLM) with smaller number of N is poor. Hence, it is preferred for the MMCCs with large number of N, while HEPWM takes precedence for relatively smaller number of N. Proposed online algorithm for the solution of HEPWM equations is presented in the next section.

IV. PROPOSED ALGORITHM

This section presents a detailed description of the proposed online algorithm (M-EO-LM), and its gradual formation from the constituent algorithms. Comparative analysis of EO with three state-of-the-art algorithms and M-EO is also provided. Furthermore, the effectiveness of the proposed M-EO-LM algorithm is proven by comparing its performance with nine state-of-the-art algorithms for twenty-nine unimodal, multimodal and composite benchmark test functions.

A. APPLICATION OF EO ALGORITHM

Recently introduced EO algorithm has found manifold applications in diverse fields, and has surpassed several state-of-the-art algorithms [23]. It follows the control volume mass balance models to reach the final equilibrium state (optimal position). It starts by randomly initializing NP number of 'particles (vectors)' within the lower and upper bounds. These particles are assembled in the matrix C and are continuously modified using (7) till the stopping criteria is met.

$$C_i = C_{eq} + (C_i - C_{eq})F + G(1-F)/(\lambda V) \tag{7}$$

where λ and V are constants, while C_{eq} represents a randomly chosen (equilibrium state) vector from a group of vectors $\{C_{eq(1)}, C_{eq(2)}, C_{eq(3)}, C_{eq(4)}, C_{eq(m)}\}$. Here, $C_{eq(1)}$ to $C_{eq(4)}$ are four particles of C with successive best fitness values, while $C_{eq(m)}$ represents their mean vector. F is an exponential term, and it maintains a balance between exploration and exploitation using (8). G defines the generation rate and it further controls the exploitation behaviour of EO by (10).

$$F = a_1 \text{sign}(r-0.5)(e^{-\lambda t} - 1) \tag{8}$$

$$t = (1 - \text{Iter}/\text{Max\_Iter})^{a_2(\text{Iter}/\text{Max\_Iter})} \tag{9}$$

$$G = G_\circ F \tag{10}$$

$$G_\circ = \text{GCP}(C_{eq} - \lambda C) \tag{11}$$

where a_1, GCP (generation rate control parameter) and a_2 are constants, and their values are determined analytically. r is a random number between 0 to 1, sign returns the sign of the term $(r-0.5)$, while Iter and Max_Iter represent the current and maximum number of iterations.

Though, EO has found hundreds of applications in diverse fields; it is employed for the first time in this article for the solution of HEPWM method. Fig. 2 presents a detailed comparison of EO, dragon fly (DF) [24], slime mould (SM) [25] and DE [26] algorithms for the solution of HEPWM method. These are soft computing (SC) methods and mostly require large number of iterations to locate a global minimum. However, present work targets rapid online solution of HEPWM method; hence, the solution process cannot be continued for large number of iterations and is required to be completed in minimum number of iterations. Fig. 2(a) depicts the convergence behavior of these algorithms in each iteration for $M = 5.15$. The solution process is continued for a maximum of one thousand iterations. EO has shown the best convergence behavior by achieving the minimum fitness value followed by SM, DE and DF algorithms. A detailed insight of convergence behaviors of these algorithms is developed by plotting the average fitness values for the range $6.76 \leq M \leq 6.86$ in Fig. 2(b). These values are obtained after a hundred solution runs of each algorithm. Clearly, EO has outclassed these algorithms by achieving the minimum average $f(\alpha)$ values (Fig. 2(b)). It has also shown a remarkable converging behavior in the first few iterations (Fig. 2(a)); but has failed to obtain the solution with targeted fitness value ($f(\alpha) \leq 10^{-4}$). Reason is its inability to avoid the local minimum, if the search space contains multiple local minima as reported in [23]. So, a modified-EO (M-EO) is formed in this work to overcome this limitation.

B. FORMATION OF M-EO ALGORITHM

M-EO is formed in the work to enhance the exploration ability and suppress the exploitation ability of EO algorithm

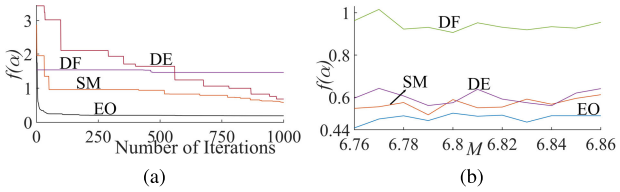

FIGURE 2. Comparison of EO, SM, DF and DE algorithms with respect to the (a) Fitness value of HEPWM equations for $M = 5.15$ in each iteration. (b) Average fitness values of HEPWM equations for $6.76 \leq M \leq 6.86$.

using (12).

$$C_i = C_{r1} + (C_{r2} - C_{r3})F \tag{12}$$

where $r1$, $r2$ and $r3$ are three random indices (ranging between 1 to NP). In (12), the last term of (7) is dropped to present a modified version of (7). Dropping of the last term subsides the exploitation ability of EO; hence, the chance of getting stuck in the local minima is lessened. Moreover, it simplifies the solution process as (10) and (11) are no more required. In addition, instead of using a constant value of a_1 and λ, both are converted into the vectors of NP number of unique randomly chosen values (between 0 to 1). Consequently, a different value of F is obtained for each vector C_i, resulting in the increased diversity of the population vectors. Furthermore, replacement of the best fitness vectors of (7) with the randomly chosen vectors in (12) enhances the exploration ability of EO. Hence, premature convergence behavior of EO is improved.

A comparison of the convergence abilities of EO and M-EO algorithms is presented in Fig. 3 through their boxplots. Boxplot provides the fitness value distribution of each particle in each iteration. Two values of M (5.15 and 5.75) are selected for this purpose. Figs. 3(a) and 3(b) show the convergence abilities of these algorithms for $M = 5.15$, while Figs. 3(c) and 3(d) depict their behaviors for $M = 5.75$ respectively. Rapid converging behavior of EO can be clearly observed in Figs. 3(a) and 3(c). However, it fails to improve the fitness after approximately forty iterations. Furthermore, required fitness value is not achieved. On contrary, scattered boxplots of M-EO outline its better exploration behavior with a compromise on convergence speed (Figs. 3(b) and 3(d)). However, required fitness value is still not achieved. A better understanding of the solution behaviors of these algorithms can be developed from a comparison of their $f(\alpha)$ values as shown in Fig. 4.

Fig. 4(a) depicts the convergence behavior of these algorithms for $M = 5.15$ in each iteration. Evidently, M-EO has shown the better response. Convergence behavior of these algorithms is further elaborated by plotting the average fitness values for the range $6.76 \leq M \leq 6.86$ in Fig. 4(b). Clearly, M-EO has outclassed EO algorithm by achieving the better fitness value (Fig. 4(b)). Hence, M-EO has appeared as the most suitable candidate (among all the presented algorithms, Figs. 2 and 4) for the solution of HEWPM method. However, similar to other algorithms (EO, SM, DF and DE), it has

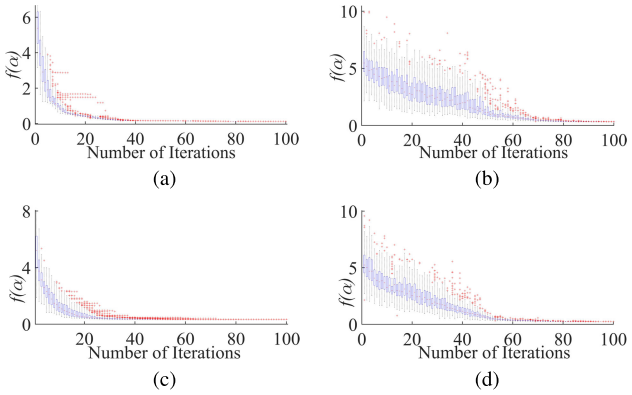

FIGURE 3. Box plot of (a) EO for $M = 5.15$. (b) M-EO for $M = 5.15$. (c) EO for $M = 5.75$. (d) M-EO for $M = 5.75$.

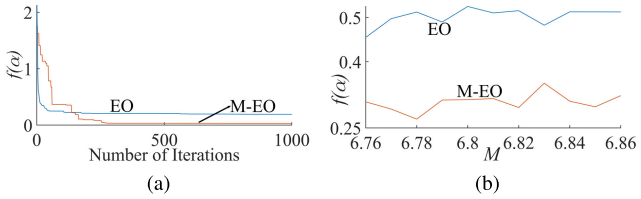

FIGURE 4. Comparison of EO and M-EO algorithms with respect to the (a) Fitness value of HEPWM equations for $M = 5.15$ in each iteration. (b) Average fitness values of HEPWM equations for $6.76 \leq M \leq 6.86$.

failed to achieve the targeted fitness value within a thousand iterations. Hence, it cannot be used to solve the HEPWM equations during the online operation, which requires the solution in few iterations. Recently, calculus based algorithms are applied conjointly with the SC or machine learning (ML) algorithms to enhance their exploitation ability, resulting in a rapid solution [12], [14], [17]. Among these, LM has cemented its prominence due to its ability to track the global minima with higher success [17], [27]. Hence, a combination of M-EO and LM (named as M-EO-LM) is proposed in this work to solve the symmetric and asymmetric HEPWM equations.

C. DESIGN OF M-EO-LM ALGORITHM

M-EO-LM algorithm is produced by blending the M-EO and LM algorithms. Fig. 4 depicts the excellent ability of the M-EO to reach near the global minima in few iterations without getting stuck in the local minima; hence it provides a good starting point for the LM algorithm. In essence, LM algorithm is a combination of gradient descent (GD) and NR algorithms [17], [27]. It utilizes the merits of both methods as GD part helps it evade the local minima while the NR part expedites the solution process. Its mathematical model is presented as:

$$C_i = C_i - \{J^T(\alpha)\epsilon(\alpha)/(J^T(\alpha)J(\alpha) + \mu I)\} \tag{13}$$

where $\epsilon(\alpha) = \{\epsilon_1, \epsilon_5, \ldots, \epsilon_k\}$ is the vector containing error function values (obtained from (1) and (2)), $J(\alpha)$ represents

the Jacobian matrix (of $\epsilon(\alpha)$) with respect to the switching angles ($\alpha_1, \alpha_2, \ldots, \alpha_N$) and I is an identity matrix of the order same as of $J(\alpha)$. μ is a constant with value varying from 0.001 to 1000, and it controls the relative contribution of GD and NR algorithms (smaller value of μ favours the NR algorithm while larger value favours GD algorithm). Normally, the initial value of μ is considered as 0.01, which is updated in each iteration by a factor of 10 or 1/10 with respect to the subsequent increase or decrease in the fitness values of the function respectively. As LM algorithm is prone to get stuck in the local minima, additional measures are required to assist the M-EO-LM algorithm in avoiding these minima. Hence, the diversity of the population vectors of the M-EO-LM algorithm is improved by replacing the redundant population vectors (population vectors with similar fitness values) with the randomly initialized vectors after every five iterations. This procedure not only enhances the exploration ability of the M-EO-LM algorithm but also ensures that it does not remain stuck in a local minimum. MATLAB implementation of the proposed M-EO-LM algorithm is presented in the following pseudo-code.

D. COMPARISON OF THE M-EO-LM ALGORITHM WITH SEVERAL STATE-OF-THE-ART ALGORITHMS

To verify the applicability of the proposed M-EO-LM algorithm for the solution of optimization problems, a detailed comparison of M-EO-LM with the algorithms proposed in [23], [28], [29], [30], [31], [32], [33], [34], and [35] namely: Equilibrium Optimizer (EO) [23], Particle Swarm Optimization (PSO) [28], Grey Wolf Optimizer (GWO) [29], Genetic Algorithm (GA) [30], Gravitational Search Algorithm (GSA) [31], Salp Swarm Algorithm (SSA) [32], Evolution Strategy with Covariance Matrix Adaptation (CMA-ES) [33], Success-History Based Parameter Adaptation Differential Evolution (SHADE) [34], and SHADE with linear population size reduction hybridized with semi-parameter adaptation of CMA-ES (LSHADE-SPACMA) [35], is presented in Table 1.

The work targets the solution of twenty-nine benchmark test functions to evaluate the performance of the proposed M-EO-LM algorithm. The benchmark test functions include seven unimodal and sixteen multimodal functions as utilized by [23], [29], [31], and [36]. Furthermore, six composite test functions (CF1 to CF6), which were introduced by [37] as challenging benchmark functions for measuring the global minima tracking ability of an optimization algorithm are also solved to verify the effectiveness of the proposed algorithm. Average (Ave) values and standard deviation (Std) values of the twenty-nine benchmark test functions obtained by the application of the M-EO-LM algorithm is presented in the column 4 of Table 1. As the comparison of EO ([23]) and rest of the algorithms ([28], [29], [30], [31], [32], [33], [34], [35]) is already carried out in [23], so the data of [23] is presented in the 5th to 13th columns (EO to LSHADE-SPACMA

Algorithm 1 Pseudo-code of the M-EO-LM Algorithm

1. Initialize the population vectors C_i ($i = 1, 2, \ldots,$ NP) in accordance with the constraint of (5),
2. Set $j = 0$ (j is the iteration number), and randomly initialize the weighting constant a_2.
3. **while** $f_i(\alpha) > 10^{-4}$ or $j <$Max_Iter (stopping criteria)
4. increment the iteration number j
5. **for** $i = 1, \ldots,$ NP
6. Calculate $f_i(\alpha)$ for each C_i vector using (1) to (5)
7. **if** $j == 1$
8. fitness_old$_i = f_i(\alpha)$
9. C_old$_i = C_i$

(where fitness_old and C_old vectors act as memory data for greedy operation of M-EO-LM algorithm)

10. save best fitness value and best vector
11. **else**
12. **if** $f_i(\alpha) <$best fitness value
13. best fitness value=$f_i(\alpha)$
14. best vector= C_i
15. **end if**
16. **if** $f_i(\alpha) <$fitness_old$_i$
17. fitness_old$_i = f_i(\alpha)$
18. C_old$_i = C_i$
19. **end if**
20. Randomly initialize the vectors a_1 and λ, and pick three unique vectors from C
21. Calculate F, t, and C_i using (8), (9) and (12)
22. **if** $f_i(\alpha) < 10^{-4}$
23. return C_i as final answer
24. **else**
25. **apply LM algorithm for ten iterations**
26. **end if-else**
27. **if** $f_i(\alpha) < 10^{-4}$
28. return C_i as the final answer
29. **end if**
30. **end if-else**
31. **end for**

The following part enhances the heterogeneity of the population vectors by replacing all but one vectors of same fitness value with the randomly initialized vectors after every five iterations.

32. **if** required solution is not obtained
33. **if** j is divisible by five
34. Replace all but one population vectors of same fitness values with the randomly initialized vectors
35. **end if**
36. **if** $j ==$ Max_Iter
37. return C_i with minimum value of $f_i(\alpha)$ as the final answer

(this loop returns C_i with minimum value of $f_i(\alpha)$ as the final answer, if the required solution is not obtained in the maximum number of iterations)

38. **end if**
39. **end if**
40. **end while**

TABLE 1. Comparison of the M-EO-LM algorithm with the algorithms of [23] for twenty-nine benchmark test functions.

Function			M−EO−LM	EO	PSO	GWO	GA	GSA	SSA	CMA−ES	SHADE	LSHADE-SPACMA
Unimodal Functions	F1	Ave	4.39E-15	3.32E-40	9.59E-06	6.59E-28	0.5549	2.53E-16	1.58E-07	1.42E-18	1.42E-09	0.2237
		Std	8.39E-17	6.78E-40	3.35E-05	1.58E-28	1.23010	9.67E-17	1.71E-07	3.13E-18	3.09E-09	0.1480
	F2	Ave	0	7.12E-23	0.0256	7.18E-17	0.0057	0.0557	2.6629	2.98E-07	0.0087	21.113
		Std	0	6.36E-23	0.0460	7.28E-17	0.0144	0.1940	1.6680	1.7889	0.0213	9.5781
	F3	Ave	1.29E-15	8.06E-09	82.2687	3.29E-06	846.34	896.53	1709.9	1.59E-05	15.435	88.775
		Std	1.77E-15	1.60E-08	97.211	1.61E-05	161.50	318.96	11242	2.21E-05	9.9489	47.230
	F4	Ave	0	5.39E-10	4.2613	5.61E-07	4.5554	7.3549	11.674	2.01E-06	0.9796	2.1170
		Std	0	1.38E-09	0.6773	1.04E-06	0.5915	1.7414	4.1792	1.25E-06	0.7995	0.4928
	F5	Ave	42.119	25.323	92.431	26.813	268.25	67.543	296.12	36.795	24.474	28.826
		Std	7.4073	0.1696	74.479	0.7933	337.69	62.225	508.86	33.461	11.208	0.8242
	F6	Ave	4.31E-15	8.29E-06	8.89E-06	0.8166	0.5625	2.5E-16	1.80E-07	6.83E-19	5.31E-10	0.2489
		Std	9.75E-17	5.02E-06	9.91E-06	0.4822	1.71977	1.74E-16	3.00E-07	6.71E-19	6.35E-10	0.1131
	F7	Ave	9.84E-5	0.0012	0.0272	0.0022	0.0429	0.0894	0.1757	0.0275	0.0235	0.0047
		Std	6.92E-5	6.54E-04	0.0080	0.0020	0.0059	0.0434	0.0629	0.0079	0.0088	0.0019
Friedman rank		mean	2.2857	2.3571	6.9286	3.7857	7.7857	7.0000	8.6429	4.3571	5.2143	6.6429
Rank			1	2	7	3	9	8	10	4	5	6
Multimodal Functions	F8	Ave	-7148.8	-9016.3	-6075.9	-6123.1	-10546	-2821.1	-7455.8	-7007.1	-11713	-3154.4
		Std	693.78	595.11	754.63	909.87	353.16	493.04	772.81	773.94	230.49	317.92
	F9	Ave	0	0	52.832	0.3105	30.823	25.968	58.371	25.338	8.5332	67.542
		Std	0	0	16.707	0.3521	7.5730	7.4701	20.016	8.5539	2.1959	10.016
	F10	Ave	8.89E-16	8.34E-14	0.0050	1.06E-13	1.6355	0.0621	2.6796	15.587	0.3957	0.0393
		Std	0	2.53E-14	0.0128	2.24E-13	0.4622	0.2363	0.8275	7.9273	0.5868	0.0151
	F11	Ave	4.83E-14	0	0.0238	0.0045	0.5611	27.702	0.0160	5.76E-15	0.0048	0.8948
		Std	1.45E-15	0	0.0287	0.0067	0.2694	5.0403	0.0112	6.18E-15	0.0077	0.1078
	F12	Ave	3.80E-3	7.97E-07	0.0276	0.0534	0.0309	1.7980	6.9915	2.87E-16	0.0346	8.18E-04
		Std	0.0126	7.69E-07	0.0540	0.0207	0.0409	0.9511	4.4175	5.64E-16	0.0875	0.0010
	F13	Ave	3.18E-3	0.0293	0.0073	0.6545	0.3622	8.8991	15.876	3.66E-04	7.32E-04	0.0102
		Std	0.0071	0.0353	0.0105	0.0045	0.3098	7.1262	16.146	0.0020	0.0028	0.0103
	F14	Ave	0.9980	0.9980	3.8490	4.0425	0.9980	5.8598	1.1965	10.237	0.9980	1.9416
		Std	5.15E-9	1.54E-16	3.2486	4.2528	4.23E-12	3.8313	0.5467	7.5445	5.83E-17	2.9633
	F15	Ave	7.51E-4	0.0024	0.0024	0.0034	0.0052	0.0037	0.0009	0.0057	0.0024	3.00E-04
		Std	2.94E-4	0.0061	0.0061	0.0062	0.0070	0.0016	0.0003	0.0121	0.0061	1.93E-19
	F16	Ave	-1.0316	-1.0316	-1.0316	-1.0316	-1.0316	-1.0316	-1.0316	-1.0316	-1.0316	-1.0316
		Std	4.75E-6	6.04E-16	6.51E-16	2.13E-08	1.34E-06	4.88E-16	6.13E-14	6.77E-16	6.51E-16	1.00E-15
	F17	Ave	0.3979	0.3979	0.3979	0.3979	0.3979	0.3979	0.3979	0.3979	0.3979	0.3979
		Std	0	0	0	2.13E-04	1.08E-05	0	3.41E-14	0	3.24E-16	0
	F18	Ave	3.0000	3.0000	3.0000	3.0000	3.0000	3.0000	3.0000	8.4000	3.0000	3.0000
		Std	1.33E-15	1.56E-15	1.97E-15	4.24E-04	4.06E-06	4.17E-15	2.20E-13	20.550	1.87E-15	1.25E-15
	F19	Ave	-3.8594	-3.8628	-3.8628	-3.8626	-3.8628	-3.8628	-3.8628	-3.8628	-3.8628	-3.8628
		Std	2.00E-5	2.59E-15	2.65E-15	0.0027	1.63E-07	2.29E-15	1.47E-10	2.7E-15	2.69E-15	2.70E-15
	F20	Ave	-3.2852	-3.2687	-3.2665	-3.2865	-3.2744	-3.3178	-3.2304	-3.2903	-3.2705	-3.2823
		Std	0.0545	0.0570	0.0603	0.1056	0.0592	0.0231	0.0616	0.0535	0.0599	0.0570
	F21	Ave	-9.9838	-8.5548	-5.9092	-8.7214	-5.7254	-5.9551	-9.6334	-5.6642	-9.2343	-9.4735
		Std	0.9223	2.7638	3.5956	2.6914	3.3262	3.7371	1.8104	3.3543	2.4153	1.7626
	F22	Ave	-10.226	-9.3353	-7.3360	-9.2415	-6.9435	-10.402	-9.0295	-8.4434	-10.148	-10.226
		Std	0.9628	2.4383	3.4738	1.6125	3.5612	2.0141	2.3911	3.3388	1.3969	0.9704
	F23	Ave	-10.535	-9.6366	-8.7482	-10.534	-7.0208	-10.536	-9.0333	-8.0750	-10.281	-10.536
		Std	1.36E-3	2.3881	2.5574	0.0012	3.8523	2.60E-15	2.9645	3.5964	1.3995	1.77E-15
Composition Functions	CF1	Ave	24.338	66.666	151.18	90.229	86.671	20.000	43.333	209.48	63.333	3.3333
		Std	43.399	95.893	123.49	105.51	97.324	48.423	67.891	215.06	80.872	18.254
	CF2	Ave	66.611	89.837	204.92	163.56	142.72	186.77	31.133	189.83	40.508	0.0000
		Std	58.281	56.366	118.89	89.476	119.58	62.726	52.149	170.79	61.462	0.0000
	CF3	Ave	160.11	161.73	273.73	210.61	214.67	218.55	235.11	274.20	139.48	104.29
		Std	34.427	33.227	110.87	95.214	73.470	117.02	80.839	213.89	33.366	14.266
	CF4	Ave	317.85	356.44	487.45	418.63	447.01	492.33	232.44	372.99	316.62	278.63
		Std	30.271	115.66	151.15	156.16	112.34	99.549	43.643	152.12	96.752	7.0670
	CF5	Ave	6.1715	52.309	214.56	143.81	91.831	232.32	27.538	224.85	39.515	2.02E-17
		Std	3.7444	95.565	180.03	149.12	73.898	75.405	41.598	286.23	51.233	7.69E-17
	CF6	Ave	495.77	768.48	794.50	837.47	811.21	845.47	628.69	845.26	684.51	540.23
		Std	33.534	192.94	175.94	136.45	173.11	80.524	184.48	139.52	201.22	122.75
Friedman rank		mean	2.6087	3.8261	6.3696	5.5652	6.1956	5.5652	5.5652	6.3696	4.0217	3.1304
Rank			1	3	7	5	6	5	5	7	4	2
							Overall results					
Friedman rank		mean	2.5862	3.5345	6.5000	5.2069	6.5690	5.7931	6.1552	5.8793	4.2241	3.9655
Rank			1	2	9	5	10	6	8	7	4	3

algorithms) of Table 1. Friedman mean rank of the algorithms is calculated based on the Ave and Std values of the functions. Finally, the algorithms are ranked in accordance with their Friedman mean ranks.

Unimodal functions (F1 to F7) are vital in evaluating the exploitation ability of an algorithm as they contain a unique minimum. It can be observed that M-EO-LM algorithm has surpassed other algorithms to locate the minimum of unimodal functions. Its Friedman mean rank is 2.2857 followed by the 2.3571 of EO algorithm. Hence, the superior exploitation ability of M-EO-LM is verified.

Multimodal functions (F8 to F23) are comprised of several local minima and a global minimum. Hence, these benchmark test functions are vital in assessing the exploration ability of the proposed M-EO-LM algorithm. Furthermore, these functions play a crucial role in evaluating the sound balance of exploitation and exploration abilities of an algorithm as it locates the global minimum by evading several local minima. In addition to the multimodal functions (F8 to F23), composite test functions (CF1 to CF6) are also utilized to evaluate the effectiveness of the algorithms. These functions imitate the search area of a complex real-life function by introducing several local minima and regions of different forms. Moreover, they are constructed by the combined applications of various mathematical operations of shifting, rotation, expansion and hybridization of five standard unimodal and multimodal mathematical functions (namely: Sphere, Rastrigin's, Weierstrass, Griewank's and Ackley's functions). Hence, they present several challenging solution tasks to the M-EO-LM and other algorithms. Readers are advised to consult [37] for further details. Clearly, M-EO-LM algorithm has shown the best results among all the algorithms for the solution of multimodal and composite test functions (Table 1). It stands at the first rank with the Friedman mean rank of 2.6087, followed by the LSHADE-SPACMA and EO algorithms with the Friedman mean rank of 3.1304 and 3.8261 respectively. Overall ranking of the algorithms is also presented by considering all the twenty-nine benchmark test functions as a single unit. M-EO-LM algorithm has shown the best results in all the (unimodal, multimodal and composite) benchmark test functions with EO algorithm taking the second place. To summarize, M-EO-LM algorithm has outperformed all the algorithms. Hence, it is established that M-EO-LM is an effective and novel algorithm, which can be utilized for any optimization problem. Application of the M-EO-LM algorithm for the offline and online solution of HEPWM method is presented in the next sections.

V. OFFLINE SIMULATION RESULTS AND DISCUSSION

In this section, switching angles varying from two to nine per quarter-cycle of output voltage are sought offline, covering the range $0.78 \leq M \leq 6.86$ for MMCC based power system. Comparison of the M-EO-LM algorithm with three state-of-the-art algorithms is reported, which depicts its superiority for the solution of HEPWM equations. Offline simulation results obtained by developing a three-phase MMCC based power system in MATLAB-Simulink are discussed. System design parameters are presented in Table 2. Purpose of the study is to present the rapid and harmonic efficient working of the proposed algorithm (M-EO-LM) based symmetric and asymmetric HEPWM methods. Furthermore, utilization of the offline results for the online solution process is discussed. A detailed comparison of the HEPWM method (using the M-EO-LM algorithm) with NLM method is also presented. Purpose of the comparison is to obtain the maximum number of angles (N) for a complete and rapid online solution of HEPWM methods using the M-EO-LM algorithm.

TABLE 2. Simulation and experimental model parameters.

Parameters	Component Values
Total SMs per-phase	8
Number of Phase	3 (Simulations), 1 (Experimental)
SM Input Voltage	10 V
Load Resistance	47 Ω
Load Inductance	5 mH
Fundamental Frequency	50 Hz

A. OFFLINE SYMMETRIC HEPWM

Fig. 5(a) displays the number of iterations taken by the proposed M-EO-LM algorithm to solve the targeted range ($0.78 \leq M \leq 6.86$), with the resolution value of M as 0.01 (subsequent value of M is obtained by incrementing the previous value by 0.01). Value of NP (population vectors) and Max_Iter (maximum iterations) are kept as $12N$ and 10 respectively for the simulations. It should be noted, transcendental nature of HEPWM method leads to the discontinuous solution angle trajectories for a particular value of N (when HEPWM angles are not available for one or more values of M). Hence, HEPWM methods with additional switching in the voltage levels are suggested in several publications to tackle this issue [8], [9], [18]. However, as an objective of this work is to present the upper limit of N for the online solution of HEPWM method, beyond which NLM should be used due to the lesser computational time of latter; the value of N is changed in the current work to mitigate the discontinuity in the solution angle trajectories for the targeted range of M ($0.78 \leq M \leq 6.86$). For instance, value of N is changed from 4 to 5 for the range $2.81 \leq M < 3.09$ (Table 3) to obtain the realizable solution angles. Remarkably, HEPWM switching angles for all values of M are obtained within two iterations (Fig. 5(a)), which asserts the exceptional convergence ability of the M-EO-LM algorithm. Furthermore, as small number of iterations are directly linked to a rapid solution process, the potential of M-EO-LM algorithm for the online solution of HEPWM method is also validated. THD values of line-to-line output voltages of MMCC for each value of M are provided in Fig. 5(b). Noticeably, IEEE-Standard of 5% THD values [19] is successfully followed for $N \geq 6$, which verifies the efficient harmonics control ability of the M-EO-LM algorithm.

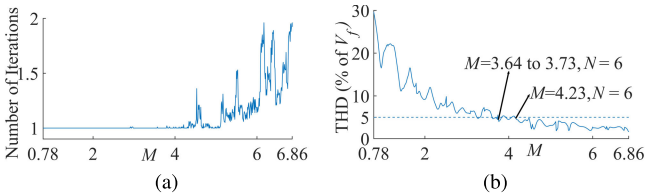

FIGURE 5. (a) Number of iterations taken by M-EO-LM to solve the HEPWM equations for the targeted range $0.78 \leq M \leq 6.86$. (b) THD values of the line-to-line output voltages for the targeted range $0.78 \leq M \leq 6.86$.

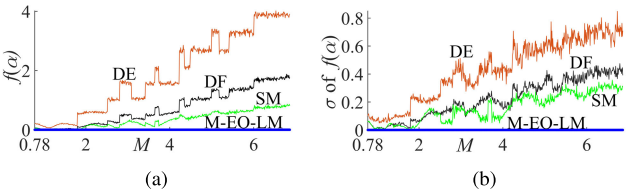

FIGURE 6. Comparison of M-EO-LM, SM, DF and DE algorithms with respect to the (a) Fitness value of HEPWM equations for $0.78 \leq M \leq 6.86$ in each iteration. (b) Standard deviation of fitness values of HEPWM equations for $0.78 \leq M \leq 6.86$.

TABLE 3. Summary of HEPWM angle trajectories for $0.78 \leq M \leq 6.86$.

N	Ranges of M	Group Number
2	$0.78 \leq M < 1.80$	G1
3	$1.80 \leq M < 2.52$	G2
4	$2.52 \leq M < 2.81$, $3.09 \leq M < 3.42$	G3, G5
5	$2.81 \leq M < 3.09$, $3.42 \leq M < 3.64$, $3.74 \leq M < 4.23$	G4, G6, G8
6	$3.64 \leq M < 3.74$, $4.35 \leq M < 4.49$	G7, G10
7	$(4.23 \leq M < 4.35$ and $4.49 \leq M < 4.56)$, $4.56 \leq M < 5.00$, $5.18 \leq M < 5.42$	G9, G11, G13
8	$5.00 \leq M < 5.18$, $5.42 \leq M < 6.01$	G12, G14
9	$6.01 \leq M < 6.335$, $6.335 \leq M < 6.76$, $6.76 \leq M \leq 6.86$	G15, G16, G17

Summary of the number of angles required to solve a particular range of M is provided in Table 3. The targeted range ($0.78 \leq M \leq 6.86$) is divided into seventeen groups (G1 to G17) such that: (i) the success rate of M-EO-LM algorithm is 100% for each value of M, and (ii) the solution angle trajectories comprising of larger range of M with smallest possible number of SMs (N) are selected (among the multiple solutions). This information is quite valuable as it directs the solution process to the relevant search space for a particular value of M. For instance, in order to operate the MMCC at $M = 5.15$, G12 of Table 3 provides the information to solve the HEPWM equations for eight angles. Moreover, Table 3 facilitates the online application of M-EO-LM algorithm for the HEPWM method, which will be discussed in section VI. Similar procedure can be adopted to obtain the low memory LUT for the online solution of all forms of HEPWM method.

Comparison of the M-EO-LM algorithm with state-of-the-art SM, DF and DE algorithms is presented in Fig. 6, with respect to their fitness function values (4). All algorithms are run a hundred times for ten iterations in each solution run, and the average and standard deviation (σ) values of their $f(\alpha)$ are shown in Figs. 6(a) and 6(b) respectively. The maximum limit of ten iterations is put as: i) the M-EO-LM algorithm has solved the HEPWM equations for the targeted range of M ($0.78 \leq M \leq 6.86$) in only two iterations (Fig. 5(a)), and ii) this is a practical limit to solve the HEPWM equations online in one fundamental time period (20 ms for the 50 Hz system). Clearly, M-EO-LM algorithm has shown superior converging behavior than the SM, DF and DE algorithms. It is the only algorithm to produce a value of zero $f(\alpha)$ (Fig. 6(a)), with $\sigma = 0$ (Fig. 6(b)) for the targeted range of M ($0.78 \leq M \leq 6.86$). Hence, the superiority of the M-EO-LM algorithm for the solution of HEPWM method is established.

Three-phase prototype of MMCC with nine SMs per-phase is designed in MATLAB-Simulink to obtain the line-to-line voltages for the pre-calculated HEPWM angles. Rapid solution behavior of the proposed M-EO-LM algorithm is depicted in the Fig. 7, which shows a smooth transition in the line-to-line output voltage of MMCC for a sudden change of M. The value of M is changed from 3.5 ($N = 5$) to 5.15 ($N = 8$) at $t = 0.3$ s. This successful response of the M-EO-LM algorithm is vital for the systems, which have dynamic requirements of the output voltage, for instance, motor drive systems. Line-to-line voltages for $M = 3.5$ (five angles) and $M = 5.15$ (eight angles) are further elaborated in Figs. 8(a) and 8(b), while their frequency spectrum are portrayed in Figs. 8(c) and 8(d) respectively. Clearly, fundamental voltage control is achieved in accordance with (3). In addition, targeted number of harmonics (sixteen and twenty-four respectively, section II) are successfully removed from the line-to-line output voltages. Furthermore, THD value for $M = 5.15$ (Fig. 8(d) is in accordance with the allowed 5% IEEE-Standard [19] limit depicting the achievement of standard harmonic control. However, filtering will be required for the output voltage of $M = 3.5$ to bring the THD value within the prescribed limits. Hence, the application of the proposed M-EO-LM algorithm for desired output voltage fundamental component and harmonics control of MMCC based power systems is pragmatic.

B. OFFLINE ASYMMETRIC HEPWM

MMCCs are not always fed with equal input voltages; hence, the solution of asymmetric HEPWM equations for the stable and efficient operation of power systems is always desirable. Solution of symmetric HEPWM equations within two iterations and with 100% success rate using M-EO-LM, furnishes the possibility of its application for the solution of asymmetric HEPWM method. To cement the pertinence of M-EO-LM algorithm for asymmetric HEPWM method; it is run a hundred times for a thousand different values M and V_m ($V_m = \text{mean}(\{V_1, V_2, \ldots, V_N\})$). The success rate turned out to be 98.01%, and the number of iterations required to solve the asymmetric HEPWM are also in line with the symmetric HEPWM method. Due to space limitations, selected values of M and relevant data are presented in Table 4.

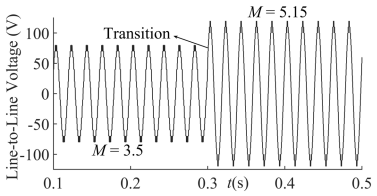

FIGURE 7. Transition of line-to-line output voltage of MMCC from $M = 3.5$ ($N = 5$) to $M = 5.15$ ($N = 8$).

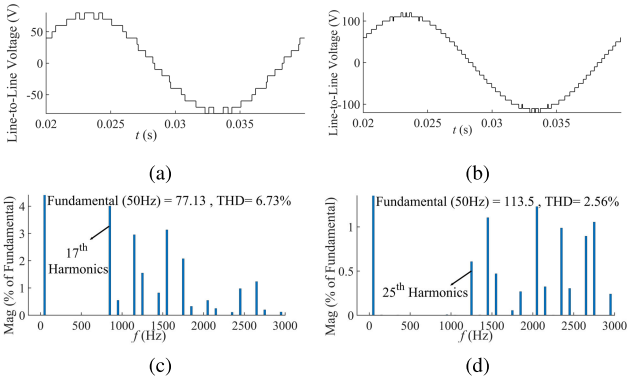

FIGURE 8. (a) Line-to-line output voltage of MMCC for $M = 3.5$. (b) Line-to-line output voltage of MMCC for $M = 5.15$. (c) FFT analysis of the output voltage for $M = 3.5$. (d) FFT analysis of the output voltage for $M = 5.15$.

Smooth transition in the asymmetric line-to-line output voltage of MMCC is shown in Fig. 9. The value of M is changed from 3.3729 ($N = 5$) to 4.9 ($N = 8$) at $t = 0.3$ s, while the magnitude of input voltages are presented in Table 5. This transition not only verifies the rapid solution ability of the proposed M-EO-LM algorithm under varying values of M but also validates its effectiveness during the change in input voltages (Table 5). As the work targets operation of MMCC based power systems with desired output voltage fundamental component and harmonics control, line-to-line voltages and the respective FFT spectrum for these values of M (3.3729 and 4.9) are portrayed in Fig. 10. Figs. 10(a) and 10(b) represent the line-to-line output voltages of MMCCs for $M = 3.3729$ and 4.9 respectively. FFT spectrum of these voltages are sequentially depicted in Figs. 10(c) and 10(d). Once again, M-EO-LM algorithm has not only established the required voltage control but has also removed the targeted harmonics (sixteen and twenty-four harmonics) from the line-to-line output voltage of MMCCs, while maintaining the THD value within the allowed 5% standard value (for $N > 5$, Fig. 10(d)). Hence, M-EO-LM algorithm is established as vital for the reliable operation of MMCCs, assuring rapid and effective voltage and frequency control response under symmetric and asymmetric conditions.

To summarize, the M-EO-LM algorithm has verified its primacy over the frequently used SC based algorithms due to its rapid and resolute convergence ability. In addition, it has successfully controlled the fundamental voltage and the harmonics during the symmetrical and asymmetrical operations, which consolidates its efficacy for the smooth and efficient operation of MMCC based power systems. Furthermore, it has led to significant progress for the online solution of HEPWM method due to the production of compact data (Table 3).

TABLE 4. Summary of selected data of asymmetric HEPWM method.

M	N	V_m	Number of Iterations
1.0460	2	0.9357	1
1.9769	3	0.9653	1
2.5473	4	0.9546	1
3.3729	5	0.9637	1.01
4.2312	6	0.9521	1.02
4.6219	7	0.9441	1.02
4.9000	8	0.9525	1.05
6.3747	9	0.9670	1.24

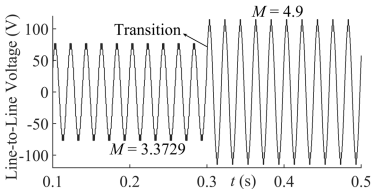

FIGURE 9. Transition of line-to-line output voltage of MMCC from $M = 3.3729$ ($N = 5$) to $M = 4.9$ ($N = 8$).

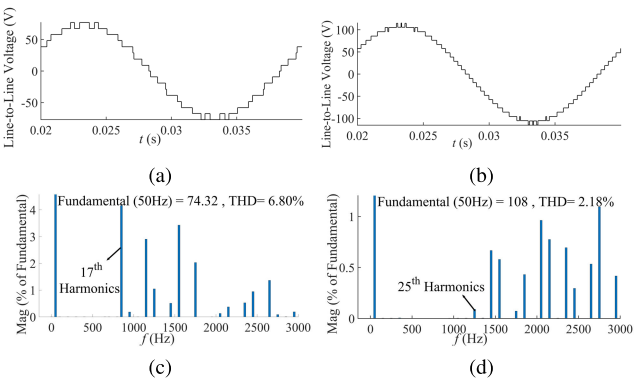

FIGURE 10. (a) Line-to-line output voltage of MMCC for $M = 3.3729$. (b) Line-to-line output voltage of MMCC for $M = 4.9$. (c) FFT analysis of the output voltage for $M = 3.3729$. (d) FFT analysis of the output voltage for $M = 4.9$.

TABLE 5. Data utilized for asymmetric MATLAB-Simulink results.

M	N	Input Voltages	V_m
3.3729	5	{0.99,0.92,0.98,0.96,0.97}	0.9640
4.9000	8	{0.99,0.92,0.98,0.96,0.97,0.95,0.91,0.94}	0.9525

C. COMPARISON OF HEPWM WITH NLM

As mentioned in section II, finding the maximum value of N for the complete online solution of HEPWM method is quite critical. Hence, a detailed comparison of the HEPWM method with the NLM method is carried out with reference to the average and maximum THD values of their line-to-line

output voltages. Switching angles for a particular value of M for the NLM method is obtained from (6), which is restated below for the ease of readers:

$$\alpha_i = \sin^{-1}[\pi(i-0.5)/(4M)], \quad i = 1, 2, \ldots, N$$

Following condition should be fulfilled to obtain the real values of α_i:

$$\pi(i-0.5)/(4M) < 1, \quad i = 1, 2, \ldots, N$$

Hence the minimum values of M ($M_{\min}$) attached with a particular value of N for the NLM method can be obtained by (14), and are provided in Table 6 (upto $N = 8$).

$$M > \pi(i-0.5)/4, \quad i = 1, 2, \ldots, N \tag{14}$$

Table 6 plays a vital role in the transition between the HEPWM and NLM methods during the online operation as it provides the value of N after which NLM should be used (in place of the HEPWM method) for the desired and rapid online output voltage fundamental component and harmonics control of MMCCs.

THD values of the line-to-line output voltages obtained using the HEPWM and NLM methods are presented in Table 7. Noticeably, HEPWM method has shown lower (average and maximum) THD values than the NLM method. However, as the mathematical model of the NLM method is simpler and its solution requires significantly less computational time than the HEPWM method, it must be preferred for the values of M showing a THD value of less than 5%. Fig. 11 shows the THD values of the line-to-line output voltages obtained using the NLM method for specific values of M. These values of M ($M \geq 5.18$) for the NLM method are picked such that the THD values are always less than the targeted 5%. Hence, the NLM method should be used for online operation of MMCCs for $M \geq 5.18$ ($N = 7$). However, Table 3 depicts that HEPWM method utilizes $N = 8$ for the range of $5.00 \leq M < 5.18$. Hence, HEPWM equations will be solved online for $N \leq 8$. To summarize, $0.78 \leq M < 5.18$ with $N \leq 8$ defines the complete range for online solution of HEPWM method, which will be targeted in the work. Solution of $M \geq 5.18$ will not be discussed as NLM can be utilized for these values. Detailed experimental results for the online implementation of HEPWM (using M-EO-LM) is provided in the subsequent section.

VI. ONLINE EXPERIMENTAL VALIDATION

Online experimental validation of the M-EO-LM algorithm for the complete solution of symmetric and asymmetric HEPWM methods is carried out by constructing a seventeen level ($N = 8$) single-phase MMCC prototype as shown in the Fig. 12. L298N modules of STMicroelectronics are utilized as the constituent SMs of MMCC. Circuit parameters are mentioned in Table 2. Switching signals for the SMs are generated using the Real-time Interface-Simulink (RTI-Simulink) package of dSPACE 1104. The objective is to employ the M-EO-LM algorithm for the online solution of HEPWM equations with minimum computational time. Online implementation and comparison of M-EO-LM algorithm with the recently published online DE-NR algorithm [14] for HEPWM method are presented in the next sections.

TABLE 6. Minimum value of M related to a particular value of N for the NLM method.

N	2	3	4	5	6	7	8
M_{min}	1.178	1.963	2.748	3.5342	4.319	5.105	5.890

TABLE 7. Comparison of HEPWM with NLM with respect to the THD values of their line-to-line output voltages.

	Maximum value of THD		Average value of THD	
N	HEPWM	NLM	HEPWM	NLM
2	29.67	31.30	17.94	15.52
3	12.01	14.34	9.317	10.16
4	8.590	10.25	6.566	7.462
5	7.230	7.680	5.600	5.766
6	4.900	6.140	4.322	4.691
7	4.480	5.030	3.460	4.004
8	3.780	4.010	2.757	3.437
9	2.840	3.700	2.525	2.990

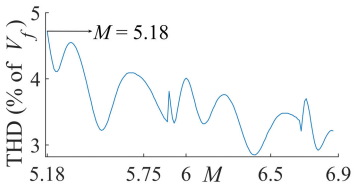

FIGURE 11. THD values of the line-to-line output voltage obtained using the NLM method for $5.18 \leq M \leq 6.86$.

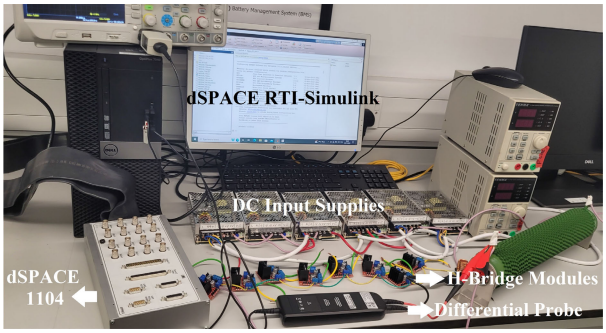

FIGURE 12. Experimental setup of the single-phase MMCC to produce the seventeen level output voltage (eight SMs).

A. ONLINE SYMMETRIC HEPWM

For the online solution of symmetric HEPWM equations, M-EO-LM algorithm is fed with the information of Table 8, while values of NP and Max_Iter are set as 3. Data of the Table 8 is obtained through the offline solution of HEPWM method (section V), and it presents the lower and upper bounds (lb and ub respectively) of each α (HEPWM switching angle). The group numbers (G1 to G12) are the same as reported by the Table 3. For instance, to obtain an output voltage for $M = 3.5$, HEPWM equations are solved online for $N = 5$ (G6 of Table 3), with the lb and ub of

α_1 to α_5 as specified by the G6 of Table 8. Clearly, Table 8 is a compact and low memory LUT (which can be easily incorporated in the code of M-EO-LM algorithm as an if-else loop). Hence, the requirement of memory for the online implementation of the M-EO-LM algorithm is trivial. Furthermore, as the Table 8 is sufficient for the online solution of HEPWM method with a high number of operating points ($0.78 \leq M < 5.18$), it eliminates the dependency on the memory burdened LUTs/parameters for the online solution of HEPWM method [12], [15], [17]. Similar online solution procedure can be adopted for all forms of HEPWM method.

Table 9 presents the computational time of M-EO-LM and DE-NR algorithms for various values of M. Computational time of the algorithm is calculated using the dSPACE 1104 real-time simulator. The algorithm is added as a function block in the dSPACE RTI-Simulink model. The model file is uploaded to the hardware controller only if the proposed algorithm can be realized in real-time; otherwise, a task overrun error is occurred. Task overrun is described as the inability of the task (algorithm) to generate the output (solution angles) before the start of the next task instance (function call), and its occurrence terminates the real-time operation. Initially, the model file is run with the sample time of 20 ms, which is continuously decreased until a particular sample time is obtained, beyond which task overrun error is generated. This sample time is the minimum time required by the algorithm to obtain the solution, and is termed as its computational time. The process is repeated to calculate the computational time of the M-EO-LM and DE-NR algorithms for each value of M, some of which are reported in the Table 9. Clearly, the computational time of M-EO-LM is quite less than the fundamental time period (20 ms for a 50 Hz system) for the targeted values of M (which can be further reduced by utilizing an optimized code, and controllers/simulators with better computational power, for instance, dSPACE 1202). Furthermore, M-EO-LM has solved the HEPWM equations faster than the DE-NR algorithm for each value of M.

Dynamic response of the system to a sudden change in the value of M from 3.8 to 3.5 ($N = 5$) is provided in the Fig. 13. Fig. 13(a) shows the variation in the symmetric HEPWM output voltage of single-phase MMCC in accordance with the change in the value of M, while the magnified transition is provided in the Fig. 13(b). Difference of the widths between the output voltages for both values of M is visible in Fig. 13(c). As expected, the output voltage levels are wider for the larger value of M ($M = 3.8$), resulting in the higher value of V_f. Noticeably, output voltage for $M = 3.5$ is shifted down in Fig. 13(c) to present a better comparison of output voltages for $M = 3.8$ and $M = 3.5$. FFT analysis of the output voltage for $M = 3.8$ is presented in Fig. 13(d). Clearly, first four non-triplens low order harmonics (5^{th}, 7^{th}, 11^{th} and 13^{th}) are successfully removed, while the fundamental voltage component is controlled according to the (3).

A step change in the values of M from 3.5 to 5.15 is displayed in Fig. 14(a), which depicts a smooth transition of single-phase symmetric output voltage from eleven levels ($M = 3.5$) to seventeen levels ($M = 5.15$) as the transition requires a computational time of only 1.1 ms (Table 9). The transition is further elaborated in Fig. 14(b) for better apprehension of the reader. Figs. 15(a) and 15(b) represent the single-phase symmetric output voltages of eleven and

TABLE 8. Look-up Table utilized for the online solution of HEPWM method using the M-EO-LM algorithm.

Group	Bounds (rad)
G1	lb = [0.0150 0.6433] ub = [0.8342 1.4625]
G2	lb = [0.2007 0.3273 0.9146] ub = [0.5847 0.9585 1.1712]
G3	lb = [0.2396 0.6029 0.8804 1.1684] ub = [0.4270 0.7908 0.9957 1.1999]
G4	lb = [0.4159 0.7156 0.8888 1.0533 1.2483] ub = [0.5727 0.8041 0.9196 1.1351 1.3291]
G5	lb = [0.0626 0.3229 0.4639 0.9448] ub = [0.1797 0.4159 0.7459 1.0965]
G6	lb = [0.0387 0.4102 0.6801 0.8299 1.2728] ub = [0.1555 0.5434 0.7306 0.9631 1.3076]
G7	lb = [0.6283 0.3737 0.8343 0.9662 1.0844 1.2669] ub = [0.6752 0.4192 0.8561 0.9742 1.1196 1.2795]
G8	lb = [0.0866 0.2313 0.4052 0.6320 1.0062] ub = [0.2324 0.3668 0.6325 1.0164 1.1114]
G9	lb = [0.3345 0.4945 0.7340 0.8840 0.9438 1.1167 1.2196] ub = [0.3708 0.5765 0.7989 0.9338 1.0270 1.1294 1.2783]
G10	lb = [0.0164 0.4929 0.6740 0.7359 0.8410 1.2297 1.3525] ub = [0.1101 0.5471 0.7240 0.8028 0.9768 1.2537 1.4361]
G11	lb = [0.1072 0.3478 0.4585 0.6780 0.8590 1.0152 1.1966] ub = [0.1940 0.4915 0.6761 0.7917 1.0172 1.1119 1.3553]
G12	lb = [0.1936 0.4570 0.6422 0.7390 0.9091 1.0363 1.1229 1.3636] ub = [0.2029 0.4745 0.6549 0.7437 0.9261 1.0376 1.1324 1.3727]

TABLE 9. Computational time of the M-EO-LM algorithm and the DE-NR algorithm for typical values of M of online symmetric HEPWM method.

N	M	Time taken (ms)	
		M-EO-LM	DE-NR
2	1.1	0.24	0.9
3	2.4	0.53	5
4	2.74	0.61	6.69
5	3.5	1.26	>20
6	3.7	0.7	>20
7	4.53	1.38	>20
8	5.15	1.1	>20

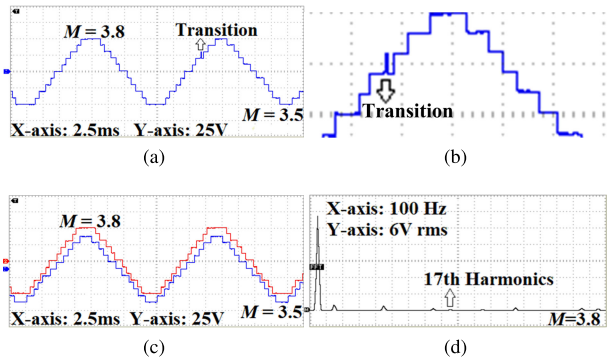

FIGURE 13. (a) Transition in the symmetric HEPWM output voltage of MMCC due to a step change of $M = 3.8$ to $M = 3.5$. (b) Zoom in transition. (c) Comparison between the widths of the output voltages for $M = 3.8$ and $M = 3.5$. (d) FFT analysis of the output voltage for $M = 3.8$.

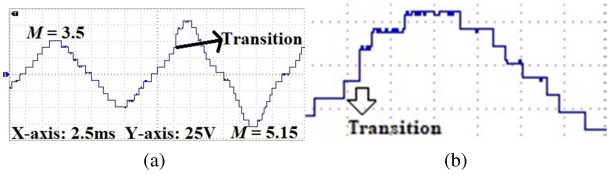

FIGURE 14. (a) Transition in the symmetric HEPWM output voltage of MMCC due to a step change of $M = 3.5$ to $M = 5.15$. (b) Zoom in transition.

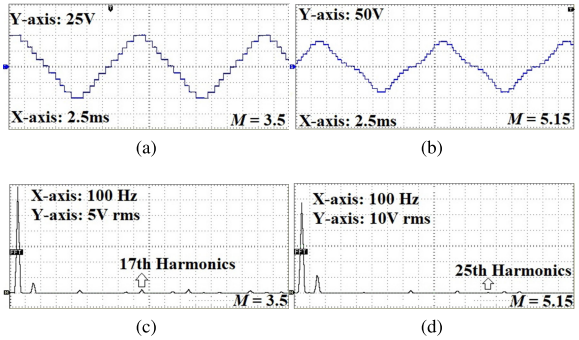

FIGURE 15. Online (a) Output voltage of MMCC for $M = 3.5$. (b) Output voltage of MMCC for $M = 5.15$. (c) FFT analysis of the output voltage for $M = 3.5$. (d) FFT analysis of the output voltage for $M = 5.15$.

seventeen level ($M = 3.5$, $N = 5$ and $M = 5.15$, $N = 8$ respectively) MMCCs respectively, while their corresponding FFT spectrum are shown in Figs. 15(c) and 15(d). Evidently, targeted 5^{th}, 7^{th}, 11^{th} and 13^{th} harmonics are successfully removed from the output voltage of MMCC for $N = 5$ (Fig. 15(c)), while 5^{th}, 7^{th}, 11^{th}, 13^{th}, 17^{th}, 19^{th} and 23^{rd} harmonics are successfully removed from the output voltage of MMCC for $N = 8$ (Fig. 15(d)). Therefore, it is concluded that the M-EO-LM algorithm can be effectively applied for a rapid and complete online solution of symmetric HEPWM method, with desired output voltage fundamental component and harmonics control.

B. ONLINE ASYMMETRIC HEPWM

Online implementation of the M-EO-LM algorithm for the asymmetric HEPWM method utilizes the information of Table 8. It further requires the real-time magnitudes of N input voltages. It is worth mentioning that the HEPWM solution angles for a particular value of M depend upon the values of input voltages ((1) to (5)). Hence, variation in the value of even a single input voltage requires the recalculation of HEPWM angles for the same value of M. Resultantly, a memory burdened solution set consisting of different HEPWM solution angles is possible for a single value of M, particularly for the systems with high number of operating points. The situation is worsened for a large range of M (for instance, $0.78 \leq M < 5.18$). The requirement of a very large LUT (or training parameters) for the online solution of asymmetric HEPWM method results in an infeasible online operation. Thus, the usage of a low memory LUT (Table 8) for the solution of asymmetric HEPWM method is of significant importance as it not only enables low memory (low cost) operation but also provide a rapid solution. Computational

TABLE 10. Computational time of the M-EO-LM algorithm and the DE-NR algorithm for typical values of M of online asymmetric HEPWM method.

N	M	V_m	Time taken (ms)	
			M-EO-LM	DE-NR
2	1.05	0.9550	0.26	1.83
3	2.28	0.9533	0.69	4.96
4	2.54	0.9300	0.6	10
5	3.3729	0.9637	1.24	>20
6	3.5458	0.9583	0.7	>20
7	4.3553	0.9614	1.38	>20
8	4.9	0.9530	1.51	>20

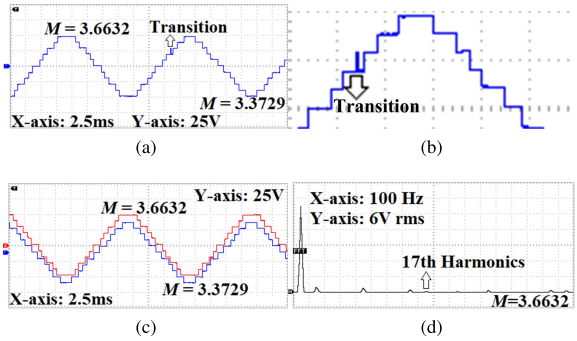

FIGURE 16. (a) Transition in the asymmetric HEPWM output voltage of MMCC due to a step change of $M = 3.6632$ to $M = 3.3729$. (b) Zoom in transition. (c) Comparison between the widths of the output voltages for $M = 3.6632$ and $M = 3.3729$. (d) FFT analysis of the output voltage for $M = 3.6632$.

time of the M-EO-LM algorithm for various values of M, corresponding to a particular value of V_m is presented in the Table 10. It can be observed that not only the computational time for each M of asymmetric HEPWM method is in line with the symmetric counterpart but also the online M-EO-LM algorithm has completely outrun the online DE-NR algorithm.

Dynamic response of the system to a sudden change in the value of M from 3.6632 to 3.3729 ($N = 5$) is provided in the Fig. 16. Fig. 16(a) shows the variation in the asymmetric HEPWM output voltage of single-phase MMCC in accordance with the change in the value of M. The magnified transition is provided in the Fig. 16(b). Difference of the widths between the output voltages for both values of M is visible in Fig. 16(c). As expected, the output voltage levels are wider for the larger value of M ($M = 3.6632$), resulting in the higher value of V_f. It should be noted, output voltage for $M = 3.3729$ is shifted down in Fig. 16(c) to present a better comparison (of output voltages) for $M = 3.6632$ and $M = 3.3729$. FFT analysis of the output voltage for $M = 3.6632$ is presented in Fig. 16(d). Clearly, first four non-triplens low order harmonics (5^{th}, 7^{th}, 11^{th} and 13^{th}) are successfully removed, while the fundamental voltage component is controlled according to the (3). Furthermore, a step change in the values of M from 3.3729 to 4.9 (with variable input voltages, Table 5) is displayed in Fig. 17. A smooth transition in the output voltage form eleven levels ($M = 3.3729$) to seventeen levels ($M = 4.9$) can be observed (Fig. 17) as the computational time required for the transition is merely 1.51 ms (Table 10). Figs. 18(a) and 18(b) represent

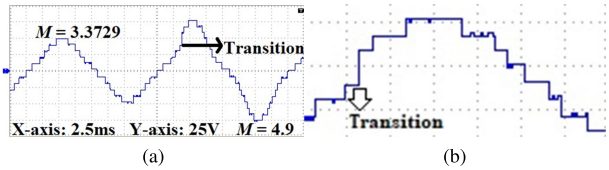

FIGURE 17. (a) Transition in the asymmetric HEPWM output voltage of MMCC due to a step change of $M = 3.3729$ to $M = 4.9$. (b) Zoom in transition.

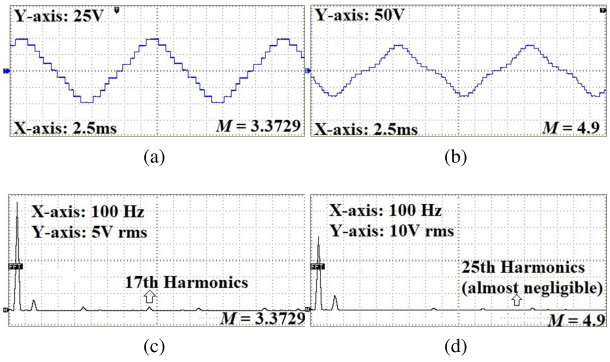

FIGURE 18. Online (a) Output voltage of MMCC for $M = 3.3729$. (b) Output voltage of MMCC for $M = 4.9$. (c) FFT analysis of the output voltage for $M = 3.3729$. (d) FFT analysis of the output voltage for $M = 4.9$.

the output voltages of eleven ($N = 5$ and $M = 3.3729$) and seventeen level ($N = 8$ and $M = 4.9$) MMCCs for asymmetric HEPWM method, while respective FFT spectrum are presented in Figs. 18(c) and 18(d). Evidently, not only the magnitude of fundamental voltage components are well controlled but also the targeted harmonics components are successfully removed. To conclude, the same values of M utilized for simulation and experimental validation produce correlated output voltage fundamental component and harmonics control. Hence, the application of the proposed online M-EO-LM algorithm for a complete solution of symmetric and asymmetric HEPWM methods for MMCC based power systems is validated.

VII. CONCLUSION

A novel online M-EO-LM algorithm is presented to solve the computationally challenging symmetric and asymmetric HEPWM equations of MMCCs. First, offline implementation of the M-EO-LM algorithm is performed for a maximum of nine ($N = 9$) HEPWM switching angle equations, which are successfully solved while controlling the fundamental voltage component and THD values of the output voltage. M-EO-LM algorithm has surpassed several state-of-the-art algorithms and has solved the targeted range ($0.78 \leq M \leq 6.86$) within only two iterations, showing its computational supremacy for the solution of arduous HEPWM method. A comparison of the HEPWM method (using the M-EO-LM algorithm) with the NLM method is carried out based on the THD values of their line-to-line output voltages to report the complete range of M ($0.78 \leq M < 5.18$ and $N = 8$) for the online solution of HEPWM method, beyond which ($M \geq 5.18$) NLM method should be preferred for the online operation of MMCCs. Secondly, a novel online framework to solve symmetric and asymmetric HEPWM methods using the proposed M-EO-LM algorithm is established. A detailed comparison of the computational times of online M-EO-LM and DE-NR algorithms are provided. The M-EO-LM algorithm has outrun the DE-NR algorithm for both the symmetric and asymmetric HEPWM methods. Simulation and online experimental results presented for the selected values of M show the pre-eminence of the proposed M-EO-LM algorithm for the complete online solution of the symmetric and asymmetric HEPWM methods. Furthermore, the optimization capability of the proposed M-EO-LM algorithm is verified by evaluating and comparing its performance with nine existing state-of-the-art algorithms for twenty-nine unimodal, multimodal and composite benchmark test functions. M-EO-LM has outperformed the existing algorithms to prove its suitability for any optimization problem.

REFERENCES

[1] H. Akagi, "Classification, terminology, and application of the modular multilevel cascade converter (MMCC)," *IEEE Trans. Power Electron.*, vol. 26, no. 11, pp. 3119–3130, Nov. 2011.
[2] A. Dekka, B. Wu, R. L. Fuentes, M. Perez, and N. R. Zargari, "Evolution of topologies, modeling, control schemes, and applications of modular multilevel converters," *IEEE J. Emerg. Sel. Topics Power Electron.*, vol. 5, no. 4, pp. 1631–1656, Dec. 2017.
[3] Z. Yang, P. Song, J. Song, X. Wang, and X. Li, "An MMC circulating current suppressing controller based on bridge arm common-mode voltage," *IEEE Access*, vol. 8, pp. 189471–189478, 2020.
[4] Z. Yang, K. Zhang, X. Li, Y. Li, and P. Song, "A control strategy for suppressing submodule capacitor voltage fluctuation of MMC based on circulating current voltage drop balance," *IEEE Access*, vol. 9, pp. 9130–9141, 2021.
[5] F. G. Turnbull, "Selected harmonic reduction in static DC–AC inverters," *IEEE Trans. Commun. Electron.*, vol. CE-83, no. 73, pp. 374–378, Jul. 1964.
[6] H. S. Patel and R. G. Hoft, "Generalized techniques of harmonic elimination and voltage control in thyristor inverters: Part I—Harmonic elimination," *IEEE Trans. Ind. Appl.*, vol. IA-9, no. 3, pp. 310–317, May 1973.
[7] H. S. Patel and R. G. Hoft, "Generalized techniques of harmonic elimination and voltage control in thyristor inverters: Part II—Voltage control techniques," *IEEE Trans. Ind. Appl.*, vol. IA-10, no. 5, pp. 666–673, Sep. 1974.
[8] M. S. A. Dahidah, G. Konstantinou, and V. G. Agelidis, "A review of multilevel selective harmonic elimination PWM: Formulations, solving algorithms, implementation and applications," *IEEE Trans. Power Electron.*, vol. 30, no. 8, pp. 4091–4106, Aug. 2015.
[9] A. M. Amjad and Z. Salam, "A review of soft computing methods for harmonics elimination PWM for inverters in renewable energy conversion systems," *Renew. Sustain. Energy Rev.*, vol. 33, pp. 141–153, May 2014.
[10] K. P. Panda, P. R. Bana, and G. Panda, "FPA optimized selective harmonic elimination in symmetric-asymmetric reduced switch cascaded multilevel inverter," *IEEE Trans. Ind. Appl.*, vol. 56, no. 3, pp. 2862–2870, May 2020.
[11] H. Zhao, T. Jin, S. Wang, and L. Sun, "A real-time selective harmonic elimination based on a transient-free inner closed-loop control for cascaded multilevel inverters," *IEEE Trans. Power Electron.*, vol. 31, no. 2, pp. 1000–1014, Feb. 2016.
[12] K. Yang, J. Hao, and Y. Wang, "Switching angles generation for selective harmonic elimination by using artificial neural networks and Quasi-Newton algorithm," in *Proc. IEEE Energy Convers. Congr. Expo. (ECCE)*, Milwaukee, WI, USA, Sep. 2016, pp. 1–5.
[13] S. Ahmad, A. Iqbal, M. Ali, K. Rahman, and A. S. Ahmed, "A fast convergent homotopy perturbation method for solving selective harmonics elimination PWM problem in multi level inverter," *IEEE Access*, vol. 9, pp. 113040–113051, 2021.
[14] A. M. Amjad, K. Mehran, S. Gadoue, and F. Blaabjerg, "Online harmonic elimination pulse width modulation technique for modular multilevel cascade converter," *Int. J. Electr. Power Energy Syst.*, vol. 133, Dec. 2021, Art. no. 107242.

[15] F. Filho, H. Z. Maia, T. H. A. Mateus, B. Ozpineci, L. M. Tolbert, and J. O. P. Pinto, "Adaptive selective harmonic minimization based on ANNs for cascade multilevel inverters with varying DC sources," *IEEE Trans. Ind. Electron.*, vol. 60, no. 5, pp. 1955–1962, May 2013.
[16] P. L. Kamani and M. A. Mulla, "Middle-level SHE pulse-amplitude modulation for cascaded multilevel inverters," *IEEE Trans. Ind. Electron.*, vol. 65, no. 3, pp. 2828–2833, Mar. 2018.
[17] J. Hao, G. Zhang, K. Yang, M. Wu, Y. Zheng, and W. Hu, "Online unified solution for selective harmonic elimination based on stochastic configuration network and Levenberg–Marquardt algorithm," *IEEE Trans. Ind. Electron.*, vol. 69, no. 10, pp. 10724–10734, Oct. 2022.
[18] K. Yang, X. Lan, Q. Zhang, and X. Tang, "Unified selective harmonic elimination for cascaded H-bridge asymmetric multilevel inverter," *IEEE J. Emerg. Sel. Topics Power Electron.*, vol. 6, no. 4, pp. 2138–2146, Dec. 2018.
[19] *IEEE Recommended Practice and Requirements for Harmonic Control in Electric Power Systems*, IEEE Standard 519, 2014.
[20] Z. Sarwer, A. Sarwar, M. Zaid, M. R. Hussan, M. Tariq, B. Alamri, and A. Alahmadi, "Implementation of a novel variable structure nearest level modulation on cascaded H-bridge multilevel inverter," *IEEE Access*, vol. 9, pp. 133974–133988, 2021.
[21] Y. Li, J. Yang, S. S. Choi, and Q. Zhao, "An analytical method to determine the optimal switching of modular multilevel converter in HVDC system," *IEEE Access*, vol. 9, pp. 13624–13635, 2021.
[22] S. Ali, J. B. Soomro, M. Mughal, F. A. Chachar, S. S. H. Bukhari, and J.-S. Ro, "Power quality improvement in HVDC MMC with modified nearest level control in real-time HIL based setup," *IEEE Access*, vol. 8, pp. 221712–221719, 2020.
[23] A. Faramarzi, M. Heidarinejad, B. Stephens, and S. Mirjalili, "Equilibrium optimizer: A novel optimization algorithm," *Knowl.-Based Syst.*, vol. 191, Mar. 2020, Art. no. 105190.
[24] S. Mirjalili, "Dragonfly algorithm: A new meta-heuristic optimization technique for solving single-objective, discrete, and multi-objective problems," *Neural Comput. Appl.*, vol. 27, no. 4, pp. 1053–1073, 2016.
[25] S. Li, H. Chen, M. Wang, A. A. Heidari, and S. Mirjalili, "Slime mould algorithm: A new method for stochastic optimization," *Future Gener. Comput. Syst.*, vol. 111, pp. 300–323, Oct. 2020.
[26] R. Storn and K. Price, "Differential evolution—A simple and efficient heuristic for global optimization over continuous spaces," *J. Global Optim.*, vol. 11, no. 4, pp. 341–359, 1997.
[27] N. Yamashita and M. Fukushima, "On the rate of convergence of the Levenberg–Marquardt method," in *Topics in Numerical Analysis* (Computing Supplementa), vol. 15, G. Alefeld and X. Chen, Eds. Vienna, Austria: Springer, 2001, doi: 10.1007/978-3-7091-6217-0_18.
[28] R. Eberhart and J. Kennedy, "A new optimizer using particle swarm theory," in *Proc. 6th Int. Symp. Micro Mach. Human Sci.*, Apr. 1995, pp. 39–43.
[29] S. Mirjalili, S. M. Mirjalili, and A. Lewis, "Grey wolf optimizer," *Adv. Eng. Softw.*, vol. 69, pp. 46–61, Mar. 2014.
[30] J. H. Holland, *Adaptation in Natural and Artificial Systems: An Introductory Analysis With Applications to Biology, Control, and Artificial Intelligence*. Cambridge, MA, USA: MIT Press, 1992.
[31] E. Rashedi, H. Nezamabadi-Pour, and S. Saryazdi, "GSA: A gravitational search algorithm," *J. Inf. Sci.*, vol. 179, no. 13, pp. 2232–2248, 2009.
[32] S. Mirjalili, A. H. Gandomi, S. Z. Mirjalili, S. Saremi, H. Faris, and S. M. Mirjalili, "Salp Swarm Algorithm: A bio-inspired optimizer for engineering design problems," *Adv. Eng. Softw.*, vol. 114, pp. 163–191, Dec. 2017.
[33] N. Hansen, S. D. Müller, and P. Koumoutsakos, "Reducing the time complexity of the derandomized evolution strategy with covariance matrix adaptation (CMA-ES)," *Evol. Comput.*, vol. 11, no. 1, pp. 1–18, Mar. 2003.
[34] R. Tanabe and A. Fukunaga, "Success-history based parameter adaptation for differential evolution," in *Proc. IEEE Congr. Evol. Comput.*, Jun. 2013, pp. 71–78.
[35] A. W. Mohamed, A. A. Hadi, A. M. Fattouh, and K. M. Jambi, "LSHADE with semi-parameter adaptation hybrid with CMA-ES for solving CEC 2017 benchmark problems," in *Proc. IEEE Congr. Evol. Comput. (CEC)*, Jun. 2017, pp. 145–152.
[36] X. Yao, Y. Liu, and G. Lin, "Evolutionary programming made faster," *IEEE Trans. Evol. Comput.*, vol. 3, no. 2, pp. 82–102, Jul. 1999.
[37] J. J. Liang, P. N. Suganthan, and K. Deb, "Novel composition test functions for numerical global optimization," in *Proc. IEEE Swarm Intell. Symp. (SIS)*, Jun. 2005, pp. 68–75.

ABDUL MOEED AMJAD received the bachelor's degree in electrical engineering from the University of Engineering and Technology Lahore, Pakistan, in 2011, and the master's degree in electrical engineering from Universiti Teknologi Malaysia, Johor Bahru, Malaysia, in 2014. He was a Lecturer with COMSATS University Islamabad (CUI), Lahore Campus, Pakistan, from 2014 to 2018. In October 2018, he joined as a Ph.D. Scholar with the School of Electronic Engineering and Computer Science (EECS), Queen Mary University of London, U.K. His research interests include modular converters, harmonic elimination PWM method, and optimization algorithms.

KAMYAR MEHRAN (Senior Member, IEEE) received the M.Sc. degree in control and automation and the Ph.D. degree in electrical and electronic engineering from Newcastle University, U.K., in 2004 and 2010, respectively. He is currently a Senior Lecturer (an Associate Professor) in electrical power engineering and the Director of the Real-Time Power and Control System (RPCS) Laboratory, School of Electronic Engineering and Computer Science (EECS), Queen Mary University of London. From 2013 to 2015, he was a Research Fellow with The University of Warwick, U.K., and from 2010 to 2013, he was a Research Associate with Newcastle University. He also acted as the commercialization manager for a university spin-off company. He has the expertise and strong track record in developing novel control methodologies and condition monitoring systems for islanded DC microgrids, energy storage systems, and SiC-based power electronics with over 80 Q1 refereed publications, and 3x book chapters. He has an extensive experience in large collaborative industrial projects and attracted £3.6M of external funding (£927k as PI) supported by Innovate U.K., Royal Society, Newton fund, EPSRC, and industry. He also collected more than eight years of professional experience in the industry. He has been an invited speaker at several conferences and companies. Before his academic career, he worked for eight years in the industry in various software-related roles.

SHADY GADOUE received the B.Sc. (Hons.) and M.Sc. degrees in electrical and electronic engineering from Alexandria University, Egypt, in 2000 and 2003, respectively, and the Ph.D. degree in power electronics and motor drives control systems from Newcastle University, Newcastle upon Tyne, U.K., in 2009. In 2011, he joined the Electrical Power Research Group, Newcastle University, as a Lecturer. In 2016, he was with the Power and Control Research Group, Imperial College London, as a full time Visiting Research Scholar. In 2017, he joined the School of Engineering and Applied Science, Aston University, Birmingham, U.K., as a Senior Lecturer. He joined the Queen Mary University of London, U.K., in 2021, as an Associate Professor, where he is currently an Associate Professor in electrical and electronic engineering with the School of Electronic Engineering and Computer Science. He has authored and coauthored more than 70 articles in the area of control and identification algorithms of power electronic converters and motor drive systems. He has been listed as one of top 2% world scientists by Stanford University, in October 2020 and October 2021, in energy engineering. His research interests include transport electrification, electric propulsion, energy systems, power electronics and their control systems, and the condition monitoring of batteries and energy storage devices for electric vehicles.